Novelty detection based on elastic wave signals measured by different techniques

Piotr Nazarko, Leonard Ziemiański

Rzeszow University of Technology
Powstańców Warszawy 12, 35-959 Rzeszów, Poland
e-mail: pnazarko@prz.edu.pl

The paper discusses the results of laboratory experiments in which three independent measurement techniques were compared: a digital oscilloscope, phased array acquisition system, a laser vibrometer 3D. These techniques take advantage of elastic wave signals actuated and sensed by a surface-mounted piezoelectric transducers as well as non-contact measurements. In these experiments two samples of aluminum strips were investigated while the damage was modeled by drilling a hole. The structure responses recorded were then subjected to a procedure of signal processing, and features' extraction was done by Principal Components Analysis. A pattern database defined was used to train artificial neural networks for the purpose of damage detection.

Keywords: Artificial neural networks, damage detection, structural health monitoring, elastic waves, non-destructive testing.

1. INTRODUCTION

The phenomenon of elastic waves propagation and its use in Non-destructive Tests and Structural Health Monitoring (SHM) systems has recently been the subject of many studies [14]. For elastic waves based SHM, contact-type transducers are typically surface mounted or fixed on test structures, but these ultrasonic techniques which rely on contact transducers suffer from the following problems: i) excitation and sensing using contact transducers are limited only to several discrete points, it is often difficult to achieve spatial resolution high enough to detect small incipient damage; ii) transducer installation and cabling can be costly and labor-intensive especially as the number of required transducers increases; iii) often the transducers and cables are vulnerable to damage and become the weakest link in the system, potentially increasing the maintenance costs; iv) for certain applications, it is not desirable to use contact transducers because the added transducers can alter the dynamic characteristics of the target structures [1]. To address these shortcomings of contact transducers, there is a strong desire to adopt non-contact laser ultrasonic techniques, which have been extensively applied in SHM [5, 6, 13]. What is an important issue in this area are sensitivity, reliability and robustness of designed systems. However, they are dependent on both the applied signal processing algorithms and reasoning procedures, as well as limitations of measurement techniques currently in use. Damage diagnosis methods can be broadly classified into two groups, data-driven methods (signal-based) and model-based methods. Data-driven approaches include the use of neural networks [12] as signal processing tools, which have proved fruitful in the context of SHM. Signal-based methods rely on various types of direct measurements. The most important issue is accurate interpretation of captured wave signals for the wave-based damage identification algorithms. However, it is quite difficult to extract this kind of damage-sensitive feature due to the complex mechanisms of wave propagation in engineering structures, even with a large number of sophisticated signal processing techniques. That is why tremendous efforts have

been directed toward identifying structural damage quantitatively through appropriate inverse algorithms, represented by artificial neural networks [15, 16]. In recent years, techniques based on multivariate statistics and neural networks have been applied to structural damage detection and a new method using the coupling of principal component analysis (PCA) and neural networks was developed.

The most common approach to recording signals of elastic wave propagation generally uses piezoelectric transducers located at certain points of the test object [11]. For this purpose, both different types of piezoelectric transducers and measuring equipment are used. In this paper, the results obtained from parallel studies using three different measurement channels were analyzed: a digital oscilloscope (LCO), phased array acquisition system (PAQ) and a 3D laser Doppler vibrometer (LDV).

Laser vibrometers allow a non-contact vibration measurement at each point of an adopted grid. Depending on the analyzed problem dealt with, vibrometers can measure the component of vibration velocity along the laser beam. For the study of elastic wave propagation phenomena scanning vibrometers (either 2D or 3D) are found to be extremely useful since they allow visualization of the structure vibration, and thus a better understanding of the phenomena that occur during the experiments. It is worth mentioning that the 3D vibrometer used in the reported studies allows determination of the components of the velocity vector (in the adopted Cartesian reference system) of elastic waves propagating in the model.

A great advantage of laser vibrometry, especially in the case of small or very slender elements, is that there is no need to mount vibration sensors and related infrastructure on the structure. On the other hand, however, it is not possible to perform the measurement at control points which are not accessible to a laser beam – this occurs when: there is no physical access to the structure, important parts of the structure are hidden behind other items, the ability of the scanned surfaces to reflect the laser light is poor.

It should be noted that elastic waves, defined as mechanical disturbances propagating inside the structure and on its surface, result in deflection of particles and their oscillations around the equilibrium position. Therefore, the signal of elastic waves propagation may vary depending on both the measuring technique used (set-up components) and the type of piezoelectric transducers used. In addition to the shape and quality of the measured signals, each of the measurement systems is also characterized by certain qualities which you need to know when planning research or purchase of selected equipment.

The scope of the study and sample results presented in this paper were designed not only to familiarize the available measurement techniques and research capabilities, but also to evaluate these signals to carry out non-destructive testing, fault detection and structural health monitoring.

2. Neural networks for novelty detection

For the purpose of comparing the effectiveness of damage detection based on the results of measurements from different measurement systems it was assumed that the assessment of the structure's state will be limited to the first level of identification, which consists of novelty detection [2, 8, 9]. In order to reduce signals dimension (see Table 1) a feature's vector was defined using a statistical algorithm that utilizes *Principal Component Analysis* (PCA) [4].

Table 1. General parameters of elastic wave signals measured by different systems.

Equipment used	Sample frequency	Signal length	Time base	Number of PCs used
LCO	5.0 MHz	25001	5 ms	16
PAQ	2.5 MHz	12500	5 ms	16
LDV	256 kHz	1024	4 ms	16

In this paper, Auto-associative Neural Networks (ANNs) were used for novelty detection. In case such trained ANN is fed with the inputs obtained from a damage state of the system, the novelty index

$$NI(\mathbf{x}) = \|\mathbf{x} - \widetilde{\mathbf{x}}\|,\tag{1}$$

which is defined as the Euclidean distance between the target input vectors $\mathbf{x}$ and the output vectors $\widetilde{\mathbf{x}}$ of the NN, will increase [2]. If the learning is successful, the index will be $NI(\mathbf{x}) \approx 0$ for data obtained from the undamaged state. However, if data is obtained from the damaged system, the novelty index will indicate an abnormal condition providing a value strongly different from zero. Although the accepted definition of a distance measure (1) seems quite simple, however, in the present task it works properly. In our opinion the main burden of fault detection lies here on ANNs since a damaged pattern should result in a network's response which is significantly different from the learned relationship.

In this task the ANNs were trained with the input vectors $\mathbf{x}$ and the output vector $\widetilde{\mathbf{x}}$ defined as

$$\mathbf{x}_{(16\times1)} = \{c_i,\, i = 1, \ldots, 16\} \to \widetilde{\mathbf{x}}_{(16\times1)} = \{c_i,\, i = 1, \ldots, 16\},\tag{2}$$

where c are the principal components calculated on the basis of time domain signals of elastic waves recorded for all damage stages (the hole's diameters).

The size of input and output layers of ANNs depends on the analyzed feature vectors and in this task was sixteen. During all the experiments performed, the ANNs were composed of a single hidden layer with three neurons. This architecture was determined taking into account the experiments conducted previously [10]. All neural networks simulations were performed in Matlab environment [7].

It is worth mentioning that learning is carried out in this case only on the basis of patterns of a specific class, for example, with the condition without damage (however, this class may also include cases of disturbances related to changing environmental conditions).

3. Laboratory tests

At the present time at least a few of techniques that enable the measurement of elastic waves propagation are already known, hence what is an interesting issue is the impact of measurement techniques used on the sensitivity and reliability of the diagnostic system designed.

To verify this issue a series of parallel tests of the same laboratory models was planned using three independent measuring circuits, which are based on the oscilloscope digital, phased array system acquisition and 3D laser vibrometer respectively.

At this preliminary stage of the study, the recorded raw signals are compared with each other for the same case of damage for the purpose of visual evaluation . The suitability assessment was indicated by the number of registered signals of properly trained classifiers and averaged values of confusion matrix calculated for the whole set of repetitions. Each set of signals was scaled to the range of -0.9 to 0.9 and then processed in the domain of principal components. The input vectors thus defined were used to train a neural network designed for an early detection of damage. Each time the ANNs training was repeated fifty times, and depending on the value of the calculated damage index (1), the classification of structure (undamaged, damaged) was made. The suitability assessment was indicated by the number of registered signals of properly trained classifiers and averaged values of confusion matrix calculated for the whole set of repetitions.

3.1. Measuring equipment

Measurements of elastic waves propagation discussed in this paper concern the experiments carried out using three different measuring devices:

- LeCroy WaveRunner digital oscilloscope (LCO),

- phased array acquisition system PAQ 16000D (PAQ),

- scanning laser Doppler vibrometer PSV-400-3D (LDV).

Each of the measuring systems created in this way is characterized by a different philosophy of measurement, but also leads to differences in the measured signals. Therefore, the main aim of the research was to show these differences on the one hand is, on the other hand, an attempt to estimate the impact of these differences on the accuracy of the failure detection system based on artificial neural networks.

3.2. Laboratory specimens

Since the main goal of this work is primarily a comparison of different measurement techniques, comparative studies were carried out on two identical samples of aluminum strips of dimensions $2000 \times 10 \times 1$ mm. One of the reasons for limiting the scope of this work to strip models was to operate at a rather simple signals (e.g. discarding the problem of multi-dimensionality, complex geometry, the presence of joints, environmental and operational conditions). The second reason is the procedure of fault detection that was developed just for strip samples (made of different materials) [3, 8, 9] and now can be examined on the signals obtained from different sources.

At one end of the model a piezoelectric transducer Mide QP22B was glued (two stacks arranged in two layers), while at the other end two transducers CMAP7 Noliac were placed (dimensions $3 \times 3 \times 2$ mm). Location of the transducers is shown schematically in Fig. 1. In these experiments, it is important to adjust the capacity of the corresponding piezoelectric transducers (and cables) to the measuring equipment used. In this case the choice of the actuators and sensors was dictated by the particular knowledge and experience acquired in the studies carried out earlier.
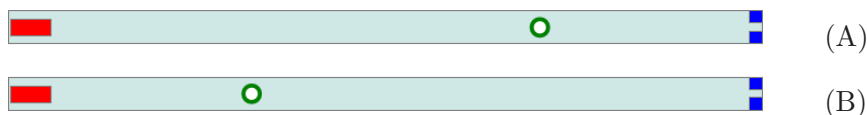
Fig. 1. Location of piezoelectric transducers in aluminum strip specimens: on the left hand side two-ply Mide QP22B and on the right hand side Noliac CMAP7 (a hole simulating damage is between).

The location of the holes whose task was to simulate the occurrence of damage in different stages is also shown. On the central axis of the band holes were drilled. Their diameter varied depending on the size of the drill used and was 1.0, 1.5, 2.0, 2.3, 2.5, 3.0, 3.2 mm. In the first case the damage was located 60 cm from the right (A), in the second 60 cm from the left end (B).

In these studies, the excitation signals in the form of five sine waves modulated with a Hanning window are used. The experiments were performed for a selected set of operating frequencies (identical for all measurement systems) of 39, 66 and 108 kHz. The frequencies are chosen in such a way that the received signals of elastic waves are as clear as possible (based on our visual assessment) and they can be measured on each of the measurement systems used. Three examples of operating frequencies were selected – below the accepted range the identified excitation wavepack and reflections from the end of the sample are superimposed on each other, while at higher frequencies the amplitude of the received signal decreased (especially in the case of the measurment setup with a digital oscilloscope the received signals became distorted and not readable – it could be caused by the type of the sensor used).

3.3. Digital oscilloscope measurements

The first measurement system consists of the following components: a wave generator, a linear amplifier, a piezoelectric transducer Mide QP22B (as an actuator and sensor), a digital oscilloscope LeCroy WaveRunner (measurement data acquisition). The devices used and glued transducer, the simulated disturbance in the form of the drilled hole and the mounting manner of the strips hanging vertically are shown in Fig. 2.
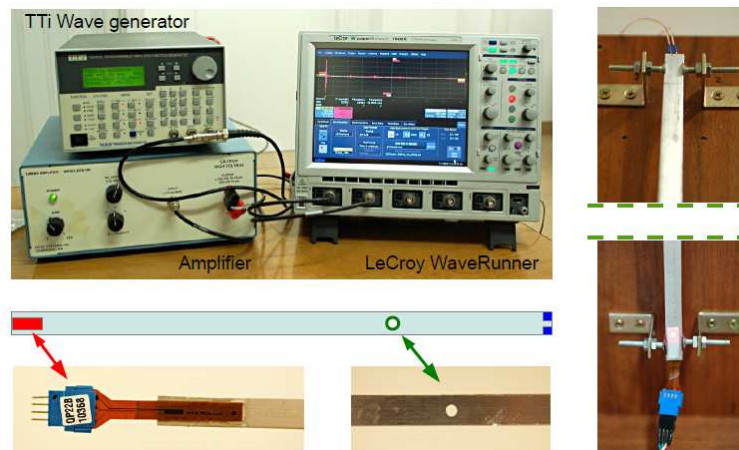
Fig. 2. Laboratory set-up with a digital oscilloscope: devices used, transmitter QP22B mounted at the model end, the hole simulating a damage, an aluminum strip support.

In the photograph of the measuring circuits it can be seen that two wires are plugged to the oscilloscope: one is responsible for the information on the pattern of the excitation signal generated (to trigger the measurement at the time of excitation appearance), while the other one plugged to one of the transmitter stacks allows recording (at the same time and place) the response to the extortion introduced.

Sample signals of elastic waves propagation recorded by a digital oscilloscope (LCO) for selected damage stages are shown in Fig. 3. The first packet of waves on these graphs is associated with the excitation introduced, and each subsequent packet is the result of propagation of the wave through the model, reflections from the end of the strip and return to the receiver (transmitter QP22B) glued to the beginning of the strip. Comparing the wave passes between them, changes in
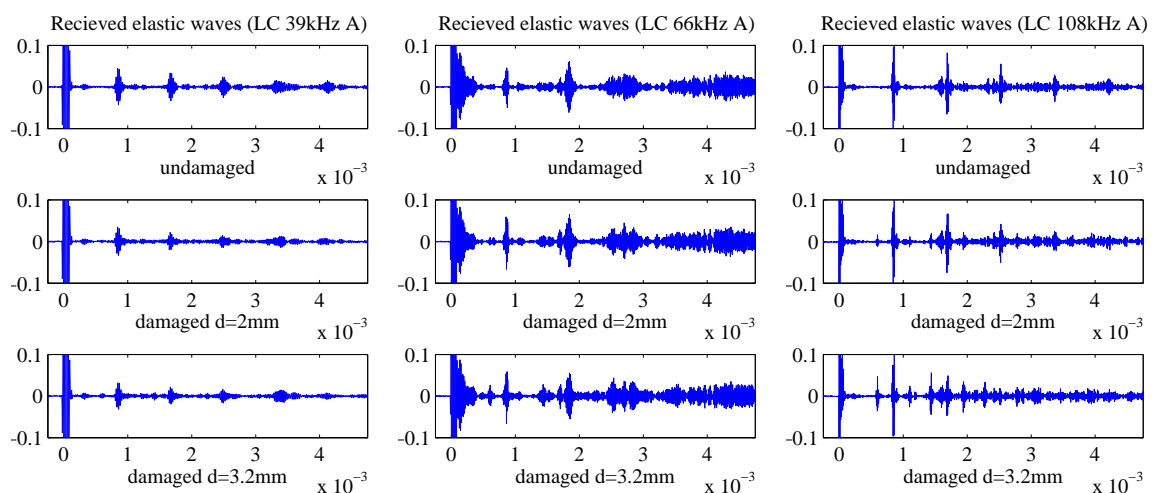
Fig. 3. Elastic wave signals recorded (LCO) in strip A at different stages of damage (no failure, damage of 2 mm in diameter, damage of 3.2 mm in diameter) and extortion frequency used.

the amplitude of wave packets as well as the appearance of additional parcels of waves (resulting from the reflection of waves from the place where the damage was located) can be observed.

It should be noted that despite the efforts at the creation of similar models, the signals recorded in models A and B are significantly different from each other in both the frequency and time of occurrence of the wave packages. There may be several reasons for this, starting with the signal generator settings (e.g., a lower frequency), through imprecise mounting of the strip on a tripod (different boundary conditions), defective sensor bonding, incidental change in the connection of the transmitter (a rotated plug changes the stack introducing the excitation pattern). Unfortunately, at this stage indication causes of these differences remains within the realm of conjecture.

As a result of the study and in spite of the differences noted, the database of signals related to two of the modeled damage positions has been established. Next, on the basis of the measured signals principal components were determined which were used as parameters describing each of time waveforms of elastic waves. Projection of the first two principal components on the principal directions is shown in Fig. 4. In this case the principal components associated with models A and B are clearly separated from each other, but it does not seem possible to separate all damaged and undamaged patterns.
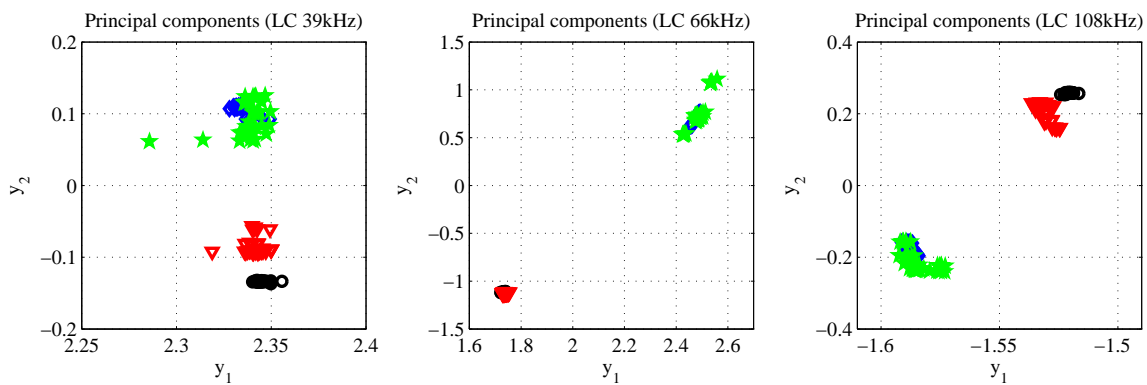
Fig. 4. Projection of the first two principal components computed for signals measured (LCO) in studied specimens (A and B) at all stages of damage growth ($\circ$ – undamaged A, $\triangledown$ – damaged A, $\diamond$ – undamaged B, $\star$ – damaged B) and extortion frequency used.

The applied principal components are used to train a structural health monitoring system whose task was to detect the damage even in the initial stage. The problem posed here can be regarded as task of pattern classification by defining two classes, for example, associated with the presence or absence of changes (damage) in the recorded signals of elastic waves. Therefore, this task illustratively consist in patterns separation on the basis of the principal components shown in Fig. 4.

All simulations of training NNs conducted on the signals measured at the studied operating frequency led to perfect classifiers. Sample results in the form of damage index (1) and division into defined classes (damaged, undamaged) are shown in Fig. 5. Although these results involve a single case (39 kHz) selected from among 50 trained replicators, in the remaining 49 cases the final results look the same. This means that the testing pattern classification accuracy is 100%. Despite the fact that the signals for other frequencies are considerably different, in consequence, they lead to similar classification results.

It should be noted here that in this kind of figures (Fig. 5) there can be found identification result for all testing patterns of both classes – without damage and damaged (each considered damage case of hole diameters of 1.0, 1.5, 2.0, 2.3, 2.5, 3.0, 3.2 mm consists of at least six patterns).

The purpose of the aforementioned scaling of the measured signals is also an attempt to assess both the energy contained in subsequent principal components and the range of novelty index values to determine the appropriate threshold level (dashed line in Fig. 5). Statistical parameters of the threshold levels on the basis of the NNs training results are summarized in Table 2. Pattern classification threshold was always taken halfway between the class of patterns without damage
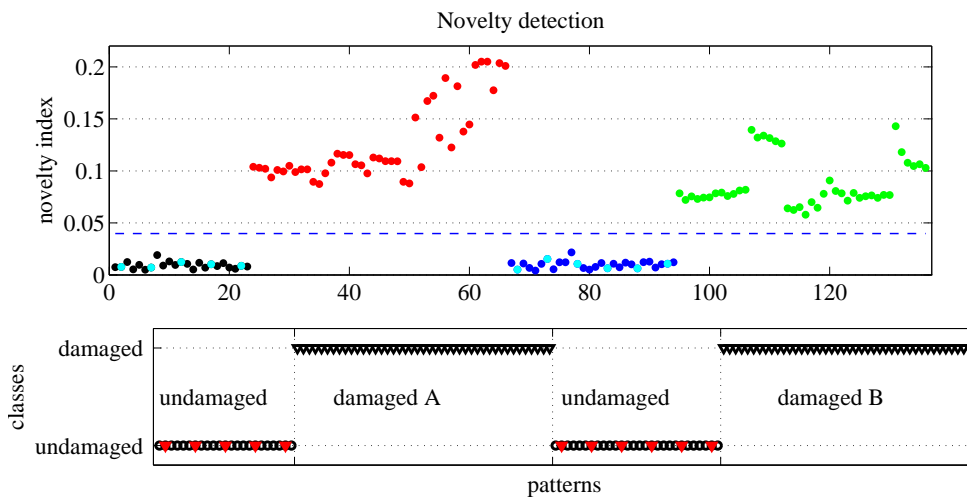
Fig. 5. Results of testing patterns classification (LCO 39 kHz) – novelty index values and distribution of defined classes.

Table 2. Statistical parameters of designated threshold level on the basis of NNs training results (LC).

Extortion	Lower range		Upper range		Threshold	
frequency	min	max	min	max	mean	std
39 kHz	0.0195	0.0264	0.0338	0.0578	**0.0308**	0.0024
66 kHz	0.0154	0.0393	0.1267	0.2480	**0.0757**	0.0104
108 kHz	0.0235	0.0655	0.0596	0.1594	**0.0479**	0.0109

and damaged. The lower range of the threshold applies to the maximum observed values of NI and the patterns without damage, while the upper range applies to the smallest values of NI and the patterns with damage. The averaged value of the threshold (mean) and its standard deviation (std) were calculated from the values adopted in subsequent repetitions of NNs training.

3.4. Phased array acquisition system measurements

The measuring setup used in the studies by PAQ system is shown in Fig. 6. In this case, one of the transducers (Noliac CMAP7) glued at the end of the strip, served as the transmitter and the other
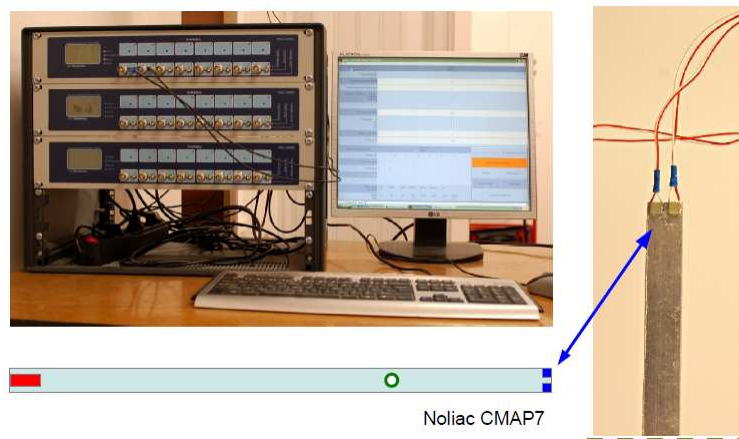
Fig. 6. Set-up with phased array acquisition system (PAQ).

as the receiver of elastic waves. It is worth noting that in comparison with transmitter QP22B which has a much larger surface area of contact and was used with the digital oscilloscope (LC, Fig. 2), piezoelectric transducer Noliac introduces and receives mainly components of the elastic wave which are normal to the plane of contact, while transducers QP22B, acting somewhat like strain gauges, can provide information about the longitudinal wave components more naturally.

The phased array acquisition system (PAQ) is a device designed for generating and recording signals of elastic waves. Each module of the system can simultaneously record up to eight signals. One of the channels can also be used to send extortion signals. Unlike the digital oscilloscope (LC), in order to receive a signal for each active input channel the extortion pattern is generated (repeated) once per channel. Although the measurement does not last long, it is not simultaneous for all sensors. In this case, repeatability of the generated extortions (e.g., its amplitude) becomes a crucial issue since without such a guarantee the diagnosis system created may have limited functionality and the initial stages of damage can be difficult to detect. By analogy with the measurements discussed previously it was assumed that in the task realized the signals registered only by one of two bonded piezoelectric transducers are used while the second transducer serves as an actuator.

However, one of the advantages of PAQ system seems to be the electronic unit generating excitation signals that cooperates well with the transducers (Noliac) of a relatively small capacity. This allows for introduction of high energy extortion signals. On the other hand, it is troublesome to obtain each time a reproducible excitation signal with the same amplitude. The obtained accuracy of the generated excitation signal ranged from one to a few percent.

Examples of elastic wave signals measured by PAQ system are presented in Fig. 7. In each of these drawings some features can be seen that distinguish the signals from one another at different stages of damage growth. However, the general difference is visible when comparing these waveforms with the corresponding signals recorded by a digital oscilloscope (Fig. 3).
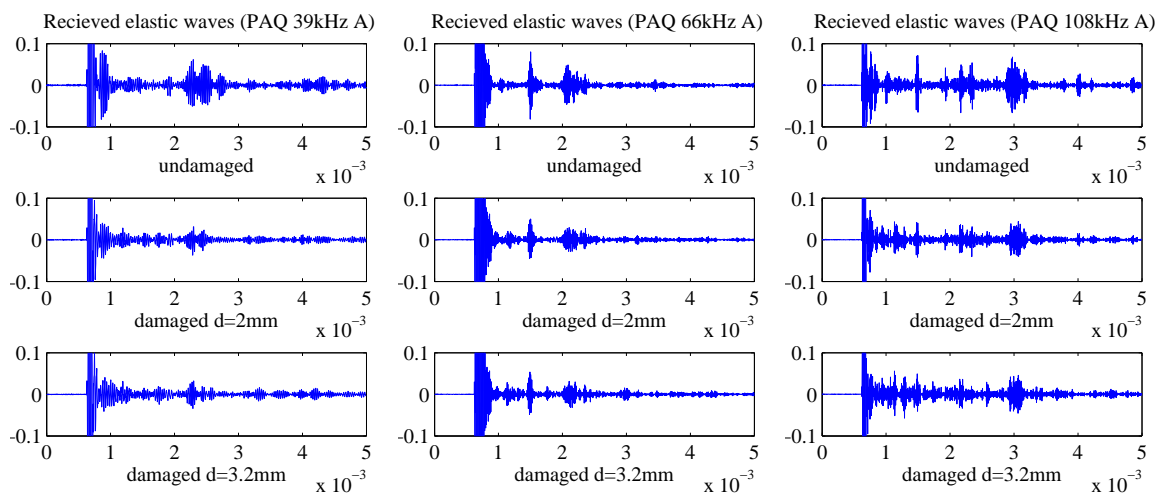
Fig. 7. Elastic wave signals recorded (PAQ) in strip A at different stages of damage (no failure, damage of 2 mm in diameter, damage of 3.2 mm in diameter) and extortion frequency used.

Similarly as before, on the basis of recorded time signals and the analysis of the principal components, corresponding damage patterns database was built. Comparing the determined values of the first two principal components (Fig. 8), the separation of patterns of the analyzed models (A and B) for signals originating from different excitation frequencies is easy to notice.

While analyzing the results of the identification process for each of the tested frequencies, it was possible to train a proper NN classifier and the separation of patterns was achieved (Fig. 9). If we compare the results of training repetitions, only in the case of the data related to the frequency of 39 kHz the efficiency of properly trained classifiers was 96%, while for frequencies of 66 and 108 kHz the effectiveness was 100%.
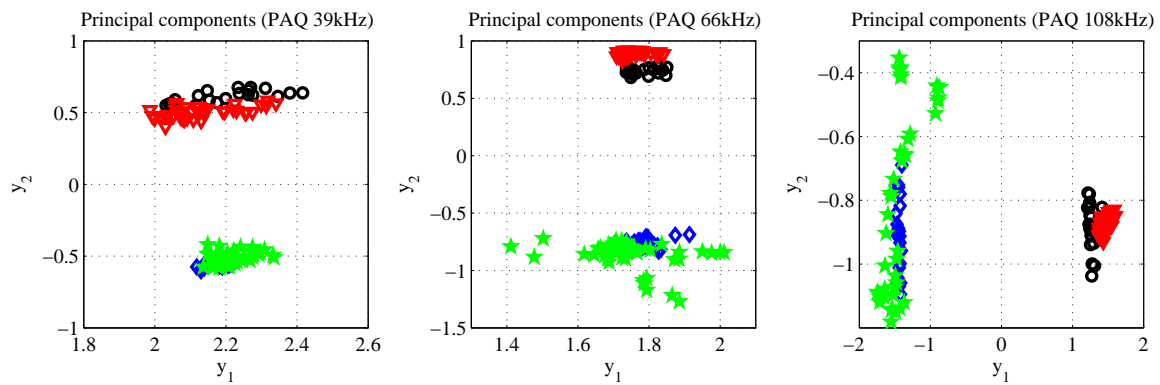
Fig. 8. Projection of the first two principal components computed for signals measured (PAQ) in studied specimens (A and B) at all stages of damage growth (∘ – undamaged A, ▽ – damaged A, ◇ – undamaged B, ⋆ – damaged B) and extortion frequency used.
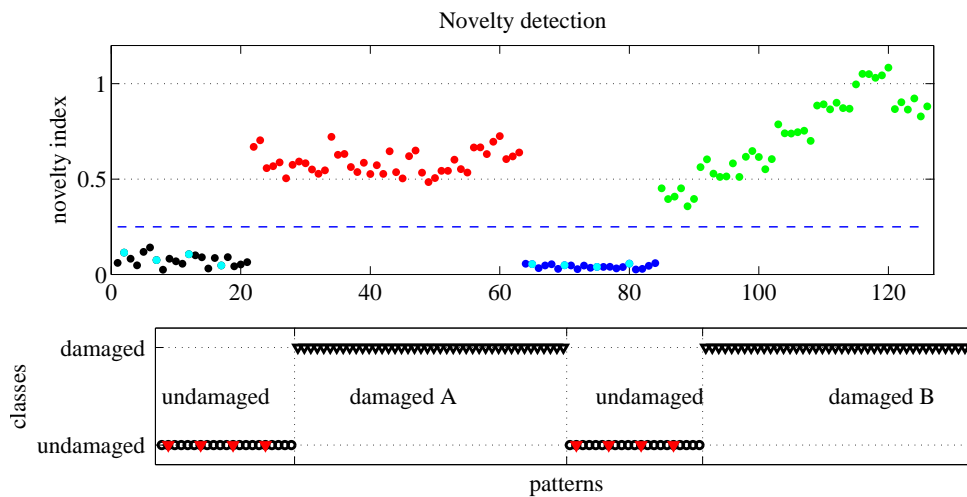
Fig. 9. Results of testing patterns classification (PAQ 39 kHz) – novelty index values and distribution of defined classes.

Similarly to the previous set of measurement data, statistical parameters of the NI and the corresponding threshold levels (that provide the proper separation of patterns) are summarized in Table 3.

Table 3. Statistical parameters of the threshold level on the basis of NNs training results (PAQ).

Extortion	Lower range		Upper range		Threshold	
frequency	min	max	min	max	mean	std
39 kHz	0.1133	0.1586	0.2201	0.4423	**0.1918**	0.0263
66 kHz	0.0923	0.0976	0.5277	0.6050	**0.3260**	0.0106
108 kHz	0.1709	0.2232	0.7244	1.1842	**0.5113**	0.0650

3.5. Laser vibrometer measurements

Another system used to measure propagation signals of elastic waves is based on a 3D laser vibrometer. In this case, excitation and generation of elastic waves is the same as that used for the measurement by a digital oscilloscope. Measurement is performed in a non-contact manner at the beginning of the band (in the position of transmitter QP22B), but on the reverse side. The laboratory set-up and the laser vibrometer used are shown in Fig. 10.
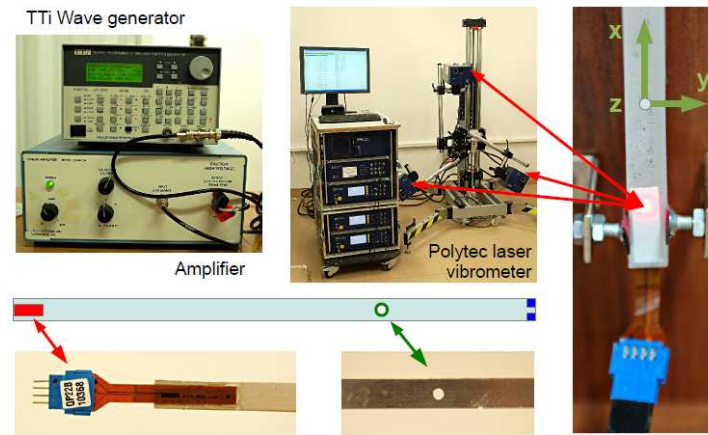
Fig. 10. Laboratory set-up with laser Doppler vibrometer (LDV).

The advantage of a 3D scanning vibrometer is obviously non-contact measurement, but in the case of the need for repeated measurements on the same object, the location of the measurement points in exactly the same measurement points is no longer so obvious. The amount of noise in the signal measurement is heavily affected by the amount of light returning to the photodetector. The quality of the reflected signal also affects the amplitude of the measured speed of the propagating elastic waves.

Another advantage of a 3D vibrometer is the ability to determine the wave velocity components in three perpendicular directions along the lines of the Cartesian reference system x, y, z. However, due to the dominant longitudinal dimension of the analyzed samples of aluminum strips, the components of the velocity vector of elastic wave propagation seem to be of little use.

While analyzing example signals registered with a laser Doppler vibrometer (velocity vectors components are shown in Fig. 11) it is much more difficult to find some features of damage occurrence and so even more its position. Although wave amplitudes were normalized to the range of $[-0.9, 0.9]$, it can still be seen that the velocity component in the plane of the model (XY) has larger values compared with the perpendicular direction (Z). On the one hand, it may actually be a result of higher speed of waves propagating in plane, but on the other hand side, it may be affected by measurement errors (e.g., projection of the velocity components) or differences in wave attenuation (between pressure and shear wave).
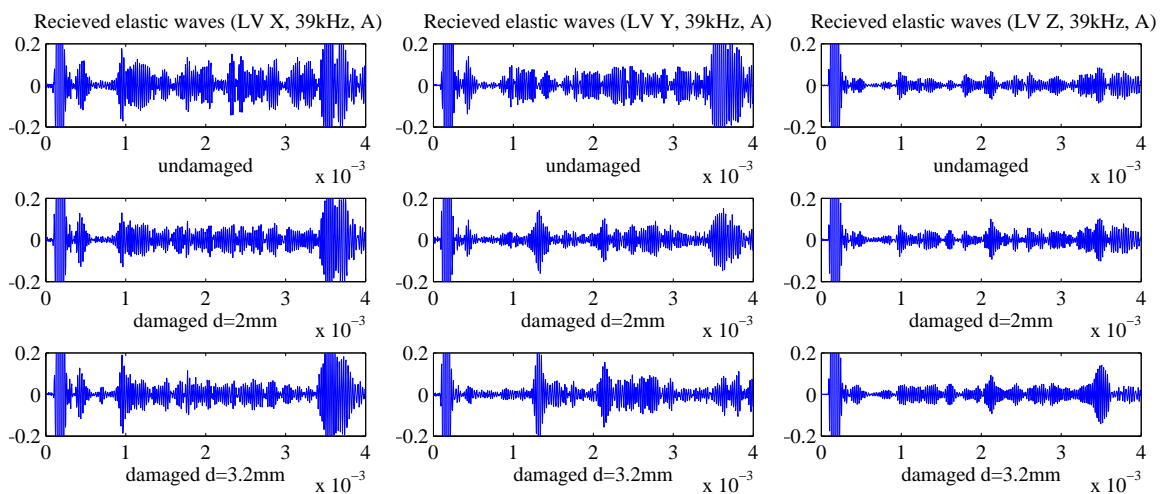
Fig. 11. Elastic wave signals recorded by laser Doppler vibrometer (LDV, X – longitudinal, Y – in plane, Z – out of plane) in strip A at different stages of damage (no failure, damage of 2 mm in diameter, damage of 3.2 mm in diameter) and extortion frequency 39 kHz.

Images of elastic waveforms for the other extortion frequencies have been omitted from this report because at this stage of the study they do not add to the conclusions already mentioned.

Based on the measured signals, the principal components have been determined (Fig. 12), which was then used to form the patterns of damage database. In comparison with the results for the other measurement systems, the distribution of patterns between models A and B on the first two principal components projections (in the XY Plane) is not as obvious as before. Only in the case of the normal component of velocity (Z direction) the distribution of patterns reproduces the scheme already known.
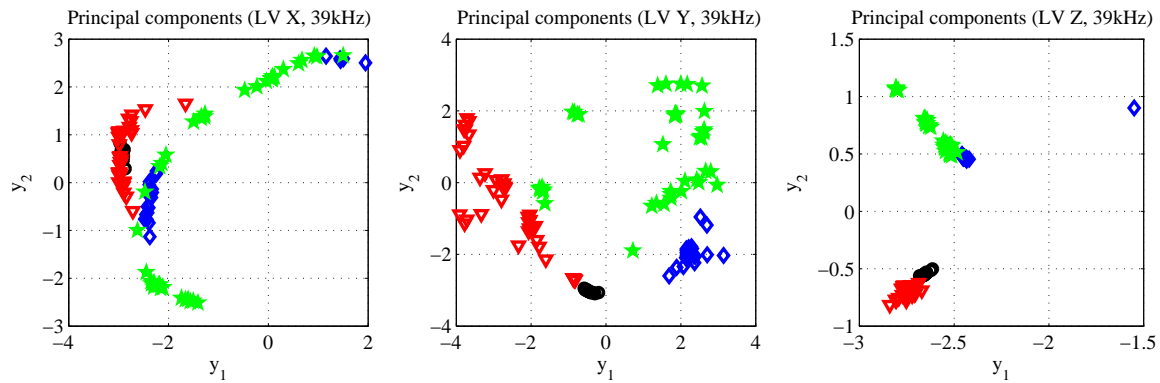
Fig. 12. Projection of the first two principal components computed for signals measured (LDV) in studied specimens (A and B) at all stages of damage growth ($\circ$ – undamaged A, $\triangledown$ – damaged A, $\diamond$ – undamaged B, $\star$ – damaged B) and extortion frequency 39 kHz.

To the task of damage detection and classification, by analogy to the previously conducted experiments, the velocity of the elastic wave signals propagating in all three directions were used. Unfortunately, not for each analyzed input vector correct results of damage classification were achieved. This applies especially to the signal components propagating in the direction of Y.

An example of the result of patterns classification for one of the properly trained classifiers and selected extortion frequency (LDV Z, 39 kHz) is shown in Fig. 13.
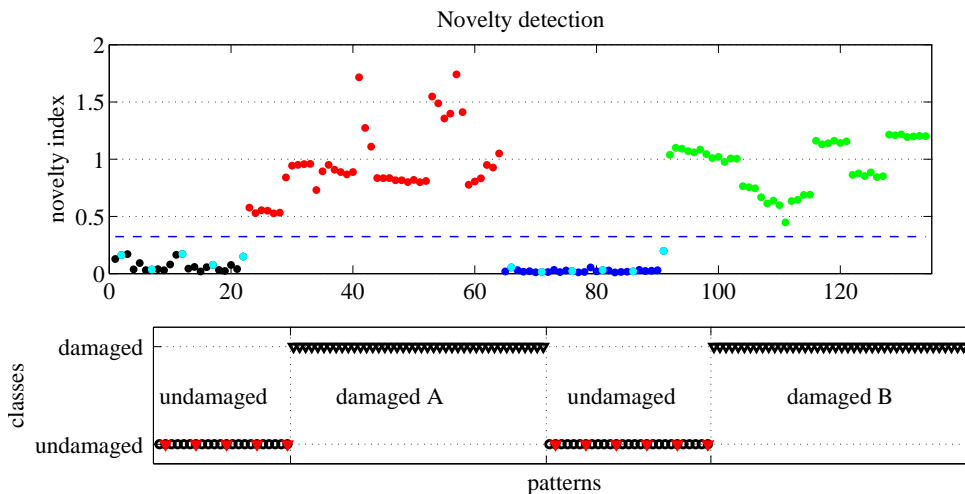
Fig. 13. The results of testing patterns classification (LDV Z, 39 kHz) – novelty index values and distribution of the defined classes.

Based on the values of NI obtained from a properly trained neural network, statistical parameters of the threshold level were determined and summarized in Table 4. It would be ideal if the average value of the threshold level was between the maximum value of the lower range and the minimum value of the upper range, unfortunately this does not hold true for any of the studied excitation frequencies.

Table 4. Statistical parameters of threshold level on the basis of NNs training results (LDV Z).

Extortion frequency	Lower range		Upper range		Threshold	
	min	max	min	max	mean	std
39 kHz	0.1706	0.3568	0.1837	0.4786	**0.2222**	0.0566
66 kHz	0.0514	0.2331	0.1770	0.4387	**0.1484**	0.0323
108 kHz	0.7465	0.9190	1.1150	1.6978	**1.1196**	0.2671

3.6. Comparison of classification results

Unfortunately, among all the trained classifiers there are some which do not lead to the expected results. In most cases, only one or a few patterns were incorrectly classified. The percentage factor of properly trained classifiers for the pattern database analyzed are summarized in Table 5. The greatest learning efficiency has been achieved for the measuring system based on a digital oscilloscope, while definitely the weakest network training results are related to the waves signals propagating in the plane of samples (X and Y directions).

Table 5. Number of classifiers trained perfectly (50 repetitions of training).

Excitation frequency	39 kHz	66 kHz	108 kHz
Digital oscilloscope LCO	100%	100%	100%
Phased array acquisition system PAQ	96%	100%	100%
Laser vibrometer LDV X (longitudinal)	76%	0%	0%
Laser vibrometer LDV Y (in plane)	0%	0%	0%
Laser vibrometer LDV Z (out of plane)	88%	98%	4%

Information on the quality of the recorded signals of elastic waves also contains a confusion matrix presented in Table 6. It contains the percentage rate of correctly classified patterns in the adopted class. In addition, the values in the table are averaged based on all the fifty performed repetitions of neural networks training. While in Table 5 it would seem that the classification based on LDV Y does not work completely, it can be seen from Table 6 that the average accuracy for the frequencies of 39 and 66 kHz was more than 75%.

Table 6. Averaged values of confusion matrix (50 repetitions of training).

Excitation frequency		39 kHz		66 kHz		108 kHz	
	True classes	Predicted classes					
		undamaged	damaged	undamaged	damaged	undamaged	damaged
LC	undamaged	100%	0%	100%	0%	100%	0%
	damaged	0%	100.0%	0%	100%	0%	100%
PAQ	undamaged	99.9%	0.1%	100%	0%	100%	0%
	damaged	2.0%	98.0%	0%	100%	0%	100%
LDV X	undamaged	99.5%	0.5%	96.0%	4.0%	94.5%	5.5%
	damaged	5.1%	94.9%	26.0%	74.0%	10.2%	89.8%
LDV Y	undamaged	98.0%	2.0%	95.8%	4.2%	97.6%	2.4%
	damaged	24.3%	75.7%	21.8%	78.2%	69.1%	30.9%
LDV Z	undamaged	99.8%	0.2%	99.9%	0.1%	96.4%	3.6%
	damaged	0.4%	99.6%	0.4%	99.6%	17.4%	82.6%

4. CONCLUSIONS AND FINAL REMARKS

Based on the research carried out some preliminary conclusions can be formulated:

- there exist such signals, for which the changes related to the appearance and growth of damage are visible and those where the changes are invisible, despite the fact that the detection of changes in the signals (caused by different factors) using neural networks can lead to very good results;

- significant differences in the signals recorded in A and B models suggest more effort should be taken in sticking of sensors and fixing the specimens;

- the approach adopted in the study does not guarantee that every time the laser spot hits the same measurement point which may partly explain the poor results obtained from the LDV measurements (the investigated models were repeatedly removed and, despite the marker placed on the model, accurate placement of the laser beam at the assumed control point is limited by a jump of the spot; another difficulty arose from the fact that in spite of properly conducted coordination of 3D system, the operating equipment warmed up, which resulted in splitting the grouped spots of the three scanning heads);

- the best patterns classification results were obtained for training the diagnosis system using the signals recorded by a digital oscilloscope (LDO).

The fault detection results may largely depend on the position of the measuring points. Therefore, further work should include an analysis of the results for different positions of the control points. Also the effect of the signals sampling frequency on damage identification results is worth considering (it was the smallest for LDV, see Table 1).

Attempts have also been made to train a neural network based on the combined information of three directions of waves propagation measured by a 3D laser vibrometer, however, the results have not been better than the classification results obtained on the basis of the LDV Z component only.

REFERENCES

[1] Y-K. An, B. Park, H. Sohn. *Complete noncontact laser ultrasonic imaging for automated crack visualization in a plate*, Smart Materials and Structures 22, 2013.

[2] M.R. Hernandez-Garcia, M. Sanchez-Silva. *Learning Machines for Structural Damage Detection.* In: Lagaros N.D., Tsompanakis Y. [Eds.] Intelligent Computational Paradigms in Earthquake Engineering. Idea Group Publishing, 2007.

[3] M. Jurek, P. Nazarko, L. Ziemiański. *Laboratory tests on elastic waves application to damage detection in metal, Plexiglas strips and composite plates.* In: Uhl T., Ostachowicz W., Holnicki-Szulc J. [Eds.] Proceedings of the Fourth European Workshop on Structural Health Monitoring, 2008.

[4] K. Kuźniar, Z. Waszczyszyn. *Neural Networks and Principal Component Analysis for Identification of Building Natural Periods.* Journal of Computing in Civil Engineering, **20**: 431–436, 2006.

[5] W.H. Leong, W.J. Staszewski, B.C. Lee, F. Scarpa. *Structural health monitoring using scanning laser vibrometry: III. Lamb waves for fatigue crack detection.* Smart Materials and Structures, **14**: 1387–1395, 2005.

[6] L. Mallet, B.C. Lee, W.J. Staszewski, F. Scarpa. *Structural health monitoring using scanning laser vibrometry: II. Lamb waves for damage detection.* Smart Materials and Structures, **13**: 261–169, 2004.

[7] MATLAB 7.2, Signal Processing Toolbox, Neural Network Toolbox.

[8] P. Nazarko and L. Ziemiański, *Towards Application of Soft Computing in Structural Health Monitoring*, in *Artificial Intelligence and Soft Computing*, LNAI 6114: 56--63, Springer-Verlag Berlin Heidelberg, 2010.

[9] P. Nazarko and L. Ziemiański, *Application of artificial neural networks in the damage identification of structural elements*, Computer Assisted Mechanics and Engineering Sciences, **18**(3): 175–189, 2011.

[10] P. Nazarko, *Soft computing methods in the analysis of elastic wave signals and damage identification*, Inverse Problems in Science and Engineering (Submitted for publication in January 2013).

[11] W. Ostachowicz, P. Kudela, P. Malinowski, T. Wandowski. *Damage localization in plate-like structures based on PZT sensors.* Mechanical Systems and Signal Processing, **23**: 1805–1829, 2009.

[12] Y. Qian, A. Mita. *Acceleration based damage indicators for building structures using neural network emulators.* Structural Control and Health Monitoring, **15**: 901–920, 2007.

[13] W.J. Staszewski, B.C. Lee, L. Mallet, F. Scarpa. *Structural health monitoring using laser vibrometry: I. Lamb wave sensing.* Smart Materials and Structures, **13**: 251–260, 2004.

[14] W.J. Staszewski, C. Boller, G. Tomlinson. Health Monitoring of Aerospace Structures: Smart Sensor Technologies and Signal Processing. John Wiley & Sons, 2004.

[15] Z. Su, L. Ye. *Lamb wave-based quantitative identification of delamination in CF/EP composite structures using artificial neural algorithm.* Composite Structures, **66**: 627–637, 2004.

[16] Z. Waszczyszyn, L. Ziemiański. *Neural networks in the identification analysis of structural mechanics problems.* In: Mroz Z., Stavroulakis G.E. [Eds.]. Parameter Identification of Materials and Structures. New York: Springer-Wien, 2005.